

Synthesis of Polymer-Derived Ceramic Si(B)CN-Carbon Nanotube Composite by Microwave-Induced Interfacial Polarization

R. Bhandavat,[†] W. Kuhn,[‡] E. Mansfield,[§] J. Lehman,[§] and G. Singh^{*,†}

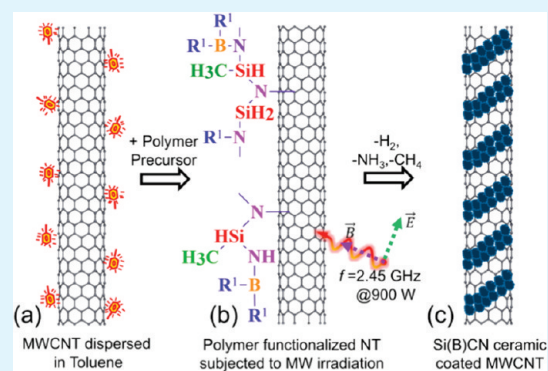
[†]Department of Mechanical and Nuclear Engineering and [‡]Department of Electrical and Computer Engineering, Kansas State University, Manhattan, Kansas 66506, United States

[§]National Institute of Standards and Technology, 325 Broadway, Boulder, Colorado 80305, United States

Supporting Information

ABSTRACT: We demonstrate synthesis of a polymer-derived ceramic (PDC)-multiwall carbon nanotube (MWCNT) composite using microwave irradiation at 2.45 GHz. The process takes about 10 min of microwave irradiation for the polymer-to-ceramic conversion. The successful conversion of polymer coated carbon nanotubes to ceramic composite is chemically ascertained by Fourier transform-infrared and X-ray photoelectron spectroscopy and physically by thermogravimetric analysis and transmission electron microscopy characterization. Frequency dependent dielectric measurements in the S-Band (300 MHz to 3 GHz) were studied to quantify the extent of microwave-CNT interaction and the degree of selective heating available at the MWCNT-polymer interface. Experimentally obtained return loss of the incident microwaves in the specimen explains the reason for heat generation. The temperature-dependent permittivity of polar molecules further strengthens the argument of internal heat generation.

KEYWORDS: microwave, polymer-derived ceramic, Si(B)CN, carbon nanotubes



1. INTRODUCTION

Carbon nanotubes (CNT) are known to possess high microwave absorbance characteristics at specific frequencies, because they couple strongly with both the electric and magnetic components of the applied external field. Temperatures as high as 2000 °C along with light emission and specimen outgassing have been reported.¹ Capitalizing on the ability of CNTs to absorb microwaves, several researchers have demonstrated (a) nanotube purification and functionalization, (b) polymer curing, (c) synthesis of monolayer graphene, and (d) electromagnetic shielding, among other applications.^{2–9}

On the basis of their broad application potential, CNT behavior has intrigued researchers to propose various microwave-CNT interaction mechanisms. Several contrasting theories have been proposed to explain the high microwave absorbance mechanism in CNTs. Wadhawan et al.¹ demonstrated that the presence of ferromagnetic catalytic impurities in CNTs are responsible for microwave absorption and also ruled out possibility of any gas adsorption and density for the microwave CNT heating. On the other hand, Walton et al.¹⁰ have shown that nanoparticles have minimal interaction with microwave at low frequencies. Further, Guo et al. proposed the relative telescopic motion between the CNT resonating tubes as the cause of heat generation.¹¹ Wu et al. experimentally concluded that the electromagnetic response of CNTs to microwaves is primarily due to dielectric properties, because they possess very weak magnetism, and the dielectric properties

are collectively or individually due to the motion of conducting electrons, relaxation, and resonance.¹² Several researchers have advanced these observations and employed CNTs as internal heat source for synthesis of CNT-polymer composites.^{6,7,9,13–16}

Polymer-derived ceramics (PDCs) of the type Si-C-N or Si-B-C-N are of interest to us because of their rheological properties in the polymer phase, ultrahigh temperature stability, and resistance to oxidation.^{17–19} The final ceramic's chemical and physical properties are known to depend on the initial molecular arrangement of the polymer precursor and processing conditions. Moreover, boron doping of PDCs results in enhanced electrical conductivity and thermoelectric power.²⁰ PDCs are amorphous ceramics prepared by controlled heating of polysilazane (SiCN) or polysiloxane (SiOC) based liquid polymeric precursors. Typically, a liquid precursor is heated to about 400 °C for cross-linking, which results in formation of an infusible polymer; followed by crushing and thermal decomposition of the infusible mass by heating it to high temperatures (~800 to 1100 °C) in inert atmospheres to yield the resulting ceramic. This method has also been utilized to prepare CNT-PDC ceramic matrix composites by either physical mixing or soaking the carbon nanotubes in liquid

Received: October 3, 2011

Accepted: December 5, 2011

Published: December 5, 2011

polymer followed by heating to convert polymer into ceramic.^{21–24} The MWCNT-Si(B)CN ceramic composite prepared by pyrolysis of a novel and single step ab initio polymer-MWCNT mix is also described in our recent work.²⁵ This route is multistep and typically consumes several hours. In this letter, we propose an alternate approach that involves microwave irradiation of polymer (boron-doped polysilazane)-coated MWCNTs. The heat generated at the polymer-CNT interface causes thermal degradation and transformation of the polymer into Si(B)CN ceramic shell that protects the nanotube core in flowing air up to at least 1000 °C.

2. EXPERIMENTAL PROCEDURE

Materials and Methods. Two sets of experiments were performed. For the first set involving microwave irradiation experiments, specimens containing equal proportions of polymeric precursor and carbon nanotubes were prepared. Briefly, the specimen preparation involved dispersion of 1 g MWCNTs (Bayer MaterialScience AG, North America) in 125 mL of toluene and sonication for 30 min, followed by dropwise addition of 5 g Si(B)CN polymeric precursor (boron-modified polyureamethylvinylsilazane) with stirring for 24 h and drying in an inert atmosphere.²⁵ The dried polymer-nanotube mix (~200 mg) was sealed in a quartz tube and exposed to full magnetron power of 900 W at 2.45 GHz (domestic microwave) for 5 min, 10 and 15 min (a total of 3 samples). Figure 1 is the

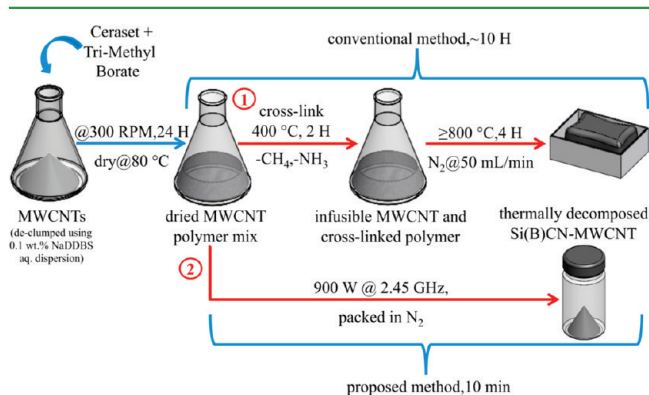


Figure 1. Experimental procedure for the synthesis of polymer-derived ceramic coated MWCNTs by (1) conventional heating method and (2) proposed method.

schematic showing the major steps involved in this process and its comparison with conventional processing of PDC composites. The other set of experiments involved dielectric measurements with vector network analyzer (VNA). For these experiments, MWCNTs (about 5 wt %) were dispersed in the polymeric precursor to obtain a polymer–CNT gel.

To ascertain the polymer to ceramic conversion, the molecular structure and bond formation of the composite was studied with X-ray photoelectron and Fourier transform infrared spectroscopy (FTIR), and results were compared with our previous work on Si(B)CN-MWCNTs composite prepared by conventional heating.²⁵ Transmission electron microscopy (TEM) was performed by use of a CM 100 microscope (Philips/FEI Corporation, Eindhoven, Holland) and Tecnai F20 XT microscope (FEI Corporation, Hillsboro, USA). X-ray photoelectron spectra were collected with a PHI Quantera SXM (ULVAC-PHI, Inc.) to study the surface chemistry of the nanocomposite by using monochromatic Al K α X-radiation

with beam size <9 μm . Following a survey scan, a 15 min high resolution scan was performed at the major elemental peaks energy window. The FTIR spectra were collected on the Thermo-Nicolet Nexus 870FT-IR from the specimen prepared by mixing approximately 1 wt % of the finely powdered specimen with FTIR grade KBr powder. TGA was performed using T.A. Instruments Q5000IR. Initial specimen weight of approximately 5 mg was heated at a rate of 10 °C/min in flowing air (25 mL/min) until the weight loss stopped and the specimen weight stabilized.

Dielectric Measurement Setup. The impedance measurements were collected from a Hewlett-Packard (HP) 8753C VNA used in combination with HP85046A for the S-Band (300 MHz to 3 GHz) at room temperature with coaxial cable (see Figure S1 in the Supporting Information). The connector (sensor) translates the variations in the permittivity of the material with the change in frequency into changes in the input impedance. The reflected line scattering parameters were then calculated from the impedance measurements obtained on the VNA over the desired frequency range (see the Supporting Information).

3. RESULTS AND DISCUSSION

Irradiation Experiments and Carbon Nanotube

Functionalization Mechanism. As expected, a large volume of outgassing was observed within a few seconds of microwave exposure, and hence a relatively small amount of material was used in large vials to avoid overpressure in the container.¹ Some sparks from the metal catalyst particles (typically present in MWCNTs) were also observed during the microwave exposure. About 50% weight loss was observed in the first five minutes of microwave exposure. The specimen did not lose weight thereafter (even after exposure to as much as 30 min). It is worth mentioning that a 30–40% weight loss is typical of PDCs prepared by conventional heating techniques. The increased weight loss in microwave-synthesized specimens could be collectively due to decomposition of the polymer into ceramic as well as burning of uncoated MWCNTs.

We propose a noncovalent sidewall functionalization of MWCNTs by the polymeric precursor, as shown in Figure 2. It is well-known that the chemical reactivity in CNTs is primarily

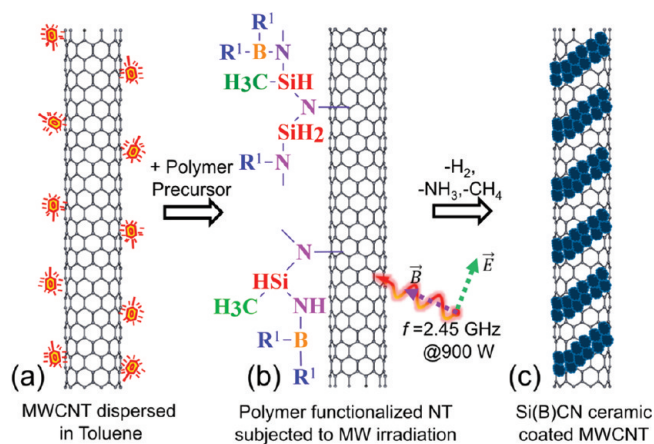


Figure 2. Symbolic illustration explaining the mechanism of noncovalent exohedral sequential sidewall functionalization of MWCNT with: (a) solvent (toluene), (b) boron-modified polysilazane polymeric precursor, and (c) pyrolyzed Si(B)CN ceramic following microwave irradiation.

due to the π orbital misalignment that exists between the adjacent carbon atoms oriented at an angle to the tube circumference.²⁶ Therefore, a strong van der Waals interaction between the aromatic group from toluene and the π - π stacking of the MWCNT sidewalls is very likely. This assists the immobilization of the polymer precursors on nanotube surfaces. Thus, a noncovalent interaction results between amine domains from the hydrophobic polymer backbone and the MWCNT sidewalls, where the former becomes the binding site. Microwave irradiation leads to selective heating of the nanotube core, resulting in thermal degradation of polymer into ceramic and thereby forming a protective coating on the nanotube surfaces. Moreover, the molecular dynamics simulations described in the literature also suggest that the concave outer surfaces of CNTs are more submissive to covalent functionalization than the inner surfaces, and hence ceramic exoskeleton is favored on the CNT surface.²⁶

Material Characterization. Electron Microscopy. Structural characterization was carried out with TEM to observe: (a) polymer distribution on nanotube surfaces before microwave exposure and (b) polymer and/or carbon nanotube decomposition (if any) after microwave irradiation was complete. After microwave exposure, the specimens showed considerable change; a more uniform amorphous coating on carbon nanotubes could be seen in the high-resolution TEM and high-angle annular dark-field (HAADF) images (Figure 3), possibly indicating polymer decomposition and ceramic

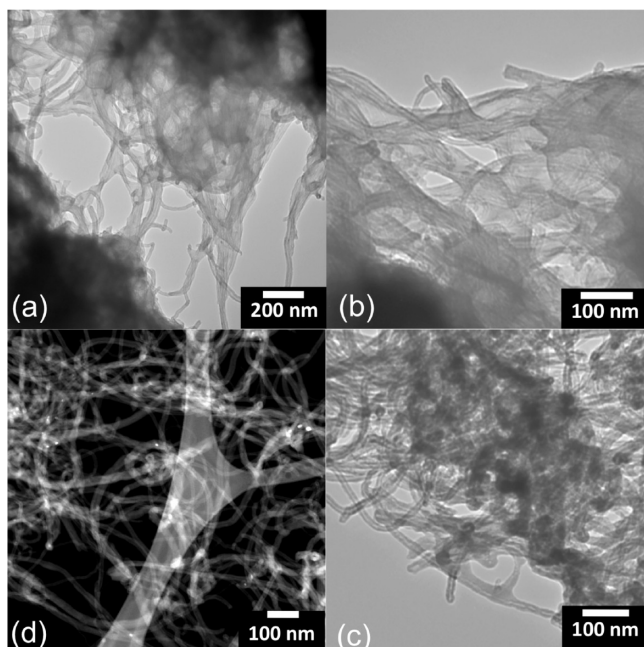


Figure 3. (a, b) TEM images showing untreated polymer-MWCNT mix. (c, d) are the conventional TEM and high-angle annular dark field (HAADF) images of Si(B)CN-MWCNTs synthesized by microwave irradiation, respectively. Note that elements with higher atomic weight (i.e., Si) appears bright in HAADF mode.

formation. The structure of the ceramic-coated CNT, including the shells and the core, was intact even for higher microwave exposure times. This is both remarkable and conclusive as the CNTs usually burn when exposed to microwave irradiation. Because both the starting polymer and resulting ceramic are amorphous (typical of PDCs), we further resorted to

spectroscopic and thermogravimetric analysis to confirm the formation of Si(B)CN ceramic.

X-ray Photoelectron Spectroscopy (XPS). XPS provides deterministic information about the nature of bond formation and the percentage of elements constituting a compound. We utilized XPS for comparing microwave irradiated specimens with those prepared by conventional heating. Comparison of the survey scans of specimens pyrolyzed at 800 °C and specimens irradiated with microwaves for 10 min consistently showed the existence of Si, B, C and N elemental peaks arising from the valence energy levels for the respective atoms (Figure 4). The resolution of each elemental peak determined the

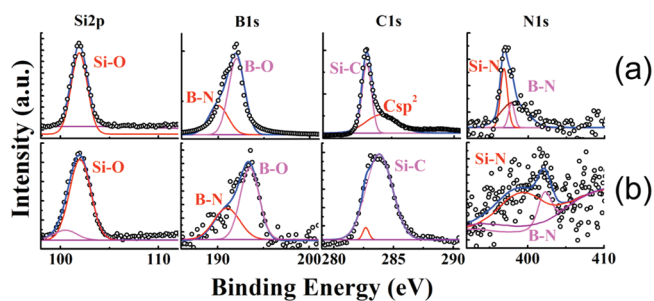


Figure 4. Core level elemental XPS spectra of Si(B)CN-MWCNT processed (a) at 800 °C for 4 h and (b) exposed to microwave for 10 min.

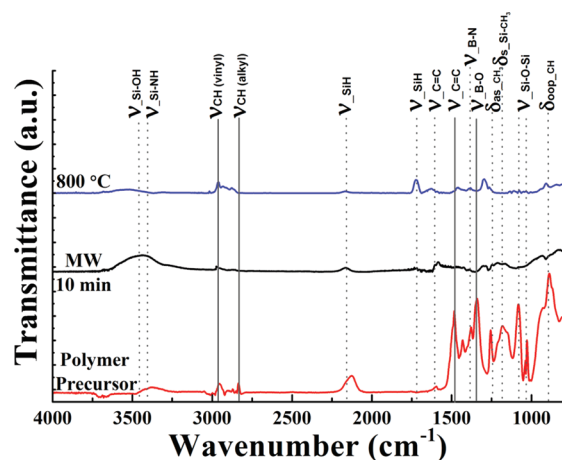
corresponding phases and their proportion in the final compound, as shown in Figure 4. The thermal degradation of the polymer and subsequent transformation to ceramic results in complementary changes in the elemental phases. Hence, XPS is critical in determining the extent of polymer conversion into ceramic. A single broad peak fitted at 102 eV observed in both specimens is due to Si–O bonds, implying the ceraset and trimethyl borate reaction and the cleavage of the methyl group from the latter. Small broad peak at lower energy at 192.5 eV is due to B–N type bond, whereas the large peak at higher energy at 195 eV is clearly due to more electronegative B–O bond as in B₂O₃. The sharp intense peak in the pyrolyzed specimen at 283 eV and the broad peak at 283.8 eV in the microwave irradiated specimen are due to Si–C, whereas the higher energy carbon peak at 284.18 eV is due to *sp*² bonded carbon. Nitrogen peaks were not very noticeable due its small fraction in the total composition; however, the Si–N bond present in the polymer backbone emerged as a prominent peak. To sum up, the XPS comparison of microwave irradiated and conventional heated specimens strongly suggests conversion of polymer precursor into ceramic by microwave irradiation.

As shown in Table 1, comparative analysis of chemical composition by XPS also revealed certain drawbacks associated with microwave assisted heating: (a) low ceramic yield (~50%) compared to that of conventional pyrolysis process (~65%), (b) lesser boron is retained in the final ceramic, probably because of high initial weight loss of the polymer, and (c) relatively high surface oxygen content in the microwave specimens. We believe that these drawbacks could be reduced or eliminated by optimizing the microwave irradiation power and exposure times as well as composition of the starting polymer.

Fourier Transform Infrared Spectroscopy (FTIR). Figure 5 is the comparison between the FTIR spectrum obtained from liquid polymer precursor, Si(B)CN-MWCNT synthesized by

Table 1. XPS Elemental and Phase Analysis Comparison of the Specimen Synthesized by Microwave Exposure for 10 min and Pyrolysis at 800 °C for 4 h

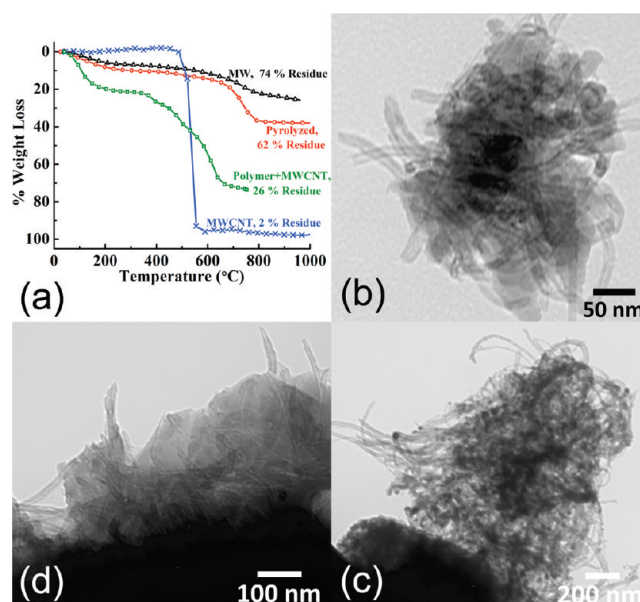
specimen	elemental ratios			estimated bonding character				
	Si/N	Si/B	B/O	Si bonds			B bonds	
				SiO ₂	SiC	Si ₃ N ₄	B ₂ O ₃	BN
microwave, 10 min	4.75	1.91	0.18	15.7	81.49	2.81	58.1	41.9
pyrolyzed, 800 °C	0.77	0.75	1.4	81.56	6.08	12.37	57.44	42.56

**Figure 5.** Diffuse reflectance spectrum of Si(B)CN-MWCNT microwave (MW) specimen, Si(B)CN-MWCNT specimen pyrolyzed at 800 °C, and the starting polymeric precursor (ν , stretching vibration mode; δ , bending vibration mode).

microwaves and the specimen synthesized by conventional pyrolysis at 800 °C. For the precursor, peaks from 2950 to 2850 and 2127 cm^{-1} correspond to C–H stretching vibration and Si–H type bond, respectively. The decrease in intensity of both these bonds in microwave irradiated specimen and the pyrolyzed specimen indicates decomposition of the polymer and subsequent ceramic formation typically observed in Si/C/N systems.²⁷ Moreover, the retention of B–O and B–N peaks at 1480 and 1380 cm^{-1} , respectively, in the processed specimens indicates retention of boron in the final ceramic (also observed in XPS analysis, Figure 4). Additional peaks at 1603 and 1457 cm^{-1} are due to C=C bonds in MWCNT. Close resemblance between the microwave irradiated and conventionally pyrolyzed specimens suggests successful ceramization as a result of heat generation due to MWCNT-microwave interactions. Additionally, the following peaks were correspondingly assigned for the Diffuse Reflectance FTIR (DRIFT) spectra collected for all the specimens: 3680 cm^{-1} , free νOH ; 3480–3400 cm^{-1} , bonded νOH in Si–OH; 3420–3390 cm^{-1} , $\nu\text{Si-NH-Si}$; 3030 cm^{-1} , terminal vinyl group on silicon $\nu\text{C-H}$; 2960 cm^{-1} , $\nu\text{as-CH}_3$; 2930 cm^{-1} , $\nu\text{as-CH}_2$; 2865 cm^{-1} , $\nu\text{s-CH}_3$; 2850 cm^{-1} , $\nu\text{s-CH}_2$; 2160 cm^{-1} , $\nu\text{Si-H}$; 1715 cm^{-1} , terminal $\nu\text{C=O}$; 1629 cm^{-1} , $\nu\text{C=O}$ [N-disubstituted amides]; 1476 cm^{-1} , $\delta\text{as-CH}_3$; 1265 cm^{-1} , $\delta\text{s-CH}_3$ [Si-CH₃]; 1396 cm^{-1} , $\nu\text{h-B-N}$; 1301 cm^{-1} , $\nu\text{B-O}$ [B(OCH₃)₃]; 1124, 1044 cm^{-1} , $\nu\text{Si-O-Si}$; 904 cm^{-1} , $\delta\text{C-H}$ out-of-plane; 808 cm^{-1} , $\delta\text{Si-H}$ (ν , stretching vibration mode; δ , bending vibration mode).

Thermogravimetric Analysis (TGA). TGA was employed to compare the high temperature stability of microwave-synthesized nanowires with those prepared through the conventional pyrolysis route. The TGA for PDC specimens processed by conventional heating route typically follows three

phases: a low-temperature weight loss due to solvent evaporation, followed by the oxidation of nonceramic coated nanotubes and other organic impurities at higher temperatures, and last the weight stabilization phase (Figure 6a). The weight loss curves for the microwave-synthesized specimen should

**Figure 6.** (a) TGA plots showing the comparative weight loss (%) for Si(B)CN-MWCNT composites synthesized by 10 min microwave irradiation (black) and conventional pyrolysis at 800 °C (red). Labels indicate respective residual weight percentages. Weight loss for ‘as obtained’ MWCNTs (blue) and ‘untreated’ polymer-MWCNT mix (green) has also been included for comparison. TGA was performed in flowing air @ 25 mL/min. Images b–d are the TEM micrographs of TGA residual corresponding to Si(B)CN-MWCNT composite synthesized by microwave irradiation.

resemble similar transitions if successful ceramization occurred during microwave exposure. As shown in the comparison plot, Figure 6a, the specimen pyrolyzed at 800 °C and the specimen synthesized by microwave exposure for ten minutes most closely resemble one another. Remarkably, the microwave specimen showed less weight loss ($25.5 \pm 3.3\%$) compared to the pyrolyzed specimen ($37.9 \pm 2.8\%$). The oxidation temperatures of both specimens were in the same temperature range. The TGA residual maintained its characteristic black color indicating survival of the nanotube core, which was later confirmed by TEM of the residual mass, Figure 6b–d. TGA analysis clearly suggests that the microwave-synthesized Si(B)CN-MWCNTs are as robust as those prepared by conventional pyrolysis methods.

The high-temperature stability of Si(B)CN-MWCNT specimens is further highlighted by comparing the TGA data with that of ‘as obtained’ MWCNT and MWCNT-polymer mix. As

shown in Figure 6a, the MWCNTs experienced ~98% weight loss at ~536 °C. The weight loss profile of nonmicrowave specimens (i.e., specimen consisting of polymer-nanotube mix) showed weight loss typical of a polysilazane precursor: (a) ~23% weight loss at ~100 °C (attributed to atmospheric absorbed moisture), (b) ~14% weight loss in 380 to 480 °C temperature range due to the release of oligomers and NH₃, and (c) a maximum weight loss of ~37% at 623.9 ± 0.6 °C, most likely due to burning the non-polymer-coated MWCNTs. Further weight loss could be due to release of CH₄ and H₂, typical of silazane-based polymers.²⁸

As shown in Table 2, because of an insignificant difference observed between the specimens processed at increasing microwave exposure times, it was concluded that (a) the

Table 2. Summary of Oxidation Temperatures and Residual Weight Obtained from TGA Analysis of Various Specimens Used in This Study

specimen	oxidation temperature (°C)	total weight loss (%)
MWCNT	536.3	97.7 ± 0.1
polymer-MWCNT	100.8 ± 2.0, 380.4 ± 1.8, 479.7 ± 1.4, 623.9 ± 0.6	73.6 ± 1.2
Si(B)CN-MWCNT 800 °C	730.0 ± 0.3	37.9 ± 2.8
Si(B)CN-MWCNT 5 min	736.8 ± 0.5	20.5 ± 3.6
Si(B)CN-MWCNT 10 min	736.2 ± 0.4	25.5 ± 3.3
Si(B)CN-MWCNT 15 min	723.7 ± 0.4	24.9 ± 3.4

polymer to ceramic conversion occurs initially within the first few minutes of microwave exposure and (b) after the initial ceramic transformation, CNT oscillation are possibly damped by the surrounding ceramic matrix.

Dielectric Measurements. To quantify the microwave interaction properties of MWCNT-polymer mix, we measured the impedance and thereby calculated the complex permittivity of the nanocomposite from 100 MHz to 3 GHz frequency. As shown in panels a and b in Figure 7, the permittivity plots for the specimen displayed a diminishing response with increasing frequency at room temperature. This behavior of permittivity corresponds to the Debye (β) relaxation phase, caused by reduced molecular polarization at the MWCNT polymer interface with increasing microwave frequency. This secondary (β) relaxation rate is temperature-dependent given by the Arrhenius relationship

$$R(T) = R_{\infty} \exp\left(\frac{-E_A}{k_B T}\right) \quad (1)$$

where R_{∞} is the relaxation rate in the high temperature limit, k_B is the Boltzmann constant, and E_A is the activation energy.²⁹ Alternatively, the Eyring relationship also gives an inverse relationship between temperature and relaxation time as

$$\tau(T) = \frac{h}{kT} \exp\left(\frac{\Delta H}{RT}\right) \exp\left(-\frac{\Delta S}{R}\right) \quad (2)$$

where h and k are Planck and Boltzmann constants, respectively, and ΔH and ΔS are the change in enthalpy and entropy, respectively.³⁰

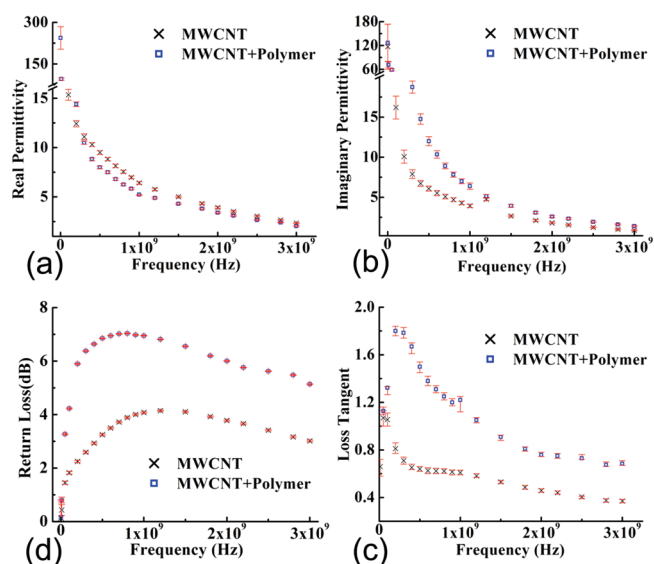


Figure 7. Dielectric properties calculated from impedance measurements: (a) Real permittivity quantifies the electrical energy the dielectric can retain; (b) imaginary permittivity determines the effectiveness to absorb microwave energy; (c) loss tangent represents the ability to effectively convert the electromagnetic energy into heat energy; and (d) return loss is a measure of effectiveness of the power delivered from the transmission line to the load for the dispersed MWCNT in polymer and agglomerated MWCNT specimens measured in the microwave frequency range from 100 MHz to 3 GHz.

We consider the MWCNT-polymer composite as a heterogeneous mix containing a small amount of conducting MWCNTs in a nonconducting polymer matrix. Under the influence of an external electromagnetic field, the charge buildup occurs at the MWCNT-polymer interface. This interfacial polarization is the cause of heat loss in the composite specimen. The MWCNT-polymer dielectric specimen, after an initial absorption of microwave energy (shown as low permittivity at room temperature in Figure 7b), experiences a temperature rise by Joule heating. This further leads to an increase in phonon vibrations, inducing dielectric and ionic conduction losses by electric carrier-phonon interactions resulting further increase in effective permittivity, ϵ'' . Moreover, for the heterogeneous dielectric material in conducting medium, the effective permittivity loss exponentially increases with temperature as given by

$$\epsilon''(\omega) = B(T) \epsilon_0 \omega^{n(T)-1} \quad (3)$$

where $B(T)$ is a temperature-dependent function at a given frequency ω .³¹ Hence, the progressively increasing permittivity leads to higher temperatures, also known as thermal runaway. Moreover, at room temperature, the induced dipole moments partially cancels out; but at higher temperatures (i.e., higher thermal energy) the molecules have greater degree of freedom and decreases the dipole canceling effect, resulting in high permittivity.²⁹ This explains the reason for high heat generation at the nanotube polymer interface sites. As shown in Figure 7d, the return loss of dispersed MWCNT in polymer is 5.6 dB at 2.45 GHz. This implies that 72.5% of incident power was dissipated as heat by the significantly lossy specimen.

As observed in Figure 7, the dispersed MWCNTs (5 wt %) in polymer showed slightly higher imaginary permittivity than the 'as obtained' nondispersed MWCNTs. In an alternating

electric field, the acquired dipole of the CNT is directed toward its length,³² and hence the CNTs dispersed in polymer may have better microwave absorption than the agglomerated CNTs. The loss tangent and return loss (Figure 7c, d) showed a similar pattern because they possess high values at low microwave frequencies and starts decreasing after ~600 MHz. This behavior could be due to more time available to π - π electron stacks at the CNT polymer interface to polarize at low frequency than at higher frequencies, where the period of electric field is significantly smaller than the relaxation time of the dipoles.¹²

4. CONCLUSION

Synthesis of PDC-MWCNT composites by microwave irradiation (in a domestic microwave oven) has been demonstrated. The most effective polymer-to-ceramic conversion occurs during the first few minutes of microwave exposure. The proposed process takes a fraction of the time required by the conventional process and hence offers an energy, time, and cost-effective alternative. The XPS surface analysis and FTIR spectral analysis of microwave specimen presents the dominance of Si-O, Si-C, B-O, and B-N bonds, analogous to that found in Si(B)CN ceramics processed at 800 °C following conventional routes. Furthermore, the high temperature oxidation resistance of microwave specimen is comparable to or better than that of Si(B)CN-MWCNT composites prepared by conventional routes as revealed by the TGA. TEM of residual TGA showed that the MWCNT structure stayed intact within the ceramic shell, further asserting the successful polymer-to-ceramic transformation.

Dielectric measurements at room temperature showed an exponentially decaying dielectric response, suggesting it to be a β -relaxation phase due to interfacial polarization. Low permittivity at 2.45 GHz suggests low energy retention, but the return loss analysis shows that about 70% of incident microwave energy on the specimen is effectively converted into heat at the polymer-nanotube interface, revealing the cause of high heat generation that leads to polymer to ceramic conversion. A similar methodology could be implemented to synthesize carbon-nanotube-based multifunctional nanocomposites with reduced processing times thereby saving energy-related costs.

■ ASSOCIATED CONTENT

Supporting Information

Description related to the dielectric measurement setup. This material is available free of charge via the Internet at <http://pubs.acs.org>.

■ AUTHOR INFORMATION

Corresponding Author

*E-mail: gurpreet@ksu.edu. Tel.: +1-785-532-7085. Fax: +1-785-532-7057.

■ ACKNOWLEDGMENTS

This research is based on work supported by the National Science Foundation under Grant EPS-0903806 and the State of Kansas through Kansas Technology Enterprise Corporation. We thank the following people for equipment usage and training: Dr. Jerry Hunter for XPS data, Myles Ikenberry and Yen Ting Kuo for the FTIR and TGA. Certain commercial equipment, instruments, or materials are identified in this

document. Such identification implies neither recommendation nor endorsement by the National Institute of Standards and Technology, or that the products identified are necessarily the best available for the purpose.

■ REFERENCES

- (1) Imholt, T. J.; Dyke, C. A.; Hasslacher, B.; Perez, J. M.; Price, D. W.; Roberts, J. A.; Scott, J. B.; Wadhawan, A.; Ye, Z.; Tour, J. M. *Chem. Mater.* **2003**, *15*, 3969.
- (2) Lin, W.; Moon, K. S.; Zhang, S. J.; Ding, Y.; Shang, J. T.; Chen, M. X.; Wong, C. P. *ACS Nano* **2010**, *4*, 1716.
- (3) Chen, Y. H.; Iqbal, Z.; Mitra, S. *Adv. Funct. Mater.* **2007**, *17*, 3946.
- (4) Chen, Y. H.; Mitra, S. *J. Nanosci. Nanotechnol.* **2008**, *8*, 5770.
- (5) Kim, W. S.; Moon, S. Y.; Park, N. H.; Huh, H.; Shim, K. B.; Ham, H. *Chem. Mater.* **2011**, *23*, 940.
- (6) Higginbotham, A. L.; Moloney, P. G.; Waid, M. C.; Duque, J. G.; Kittrell, C.; Schmidt, H. K.; Stephenson, J. J.; Arepalli, S.; Yowell, L. L.; Tour, J. M. *Compos. Sci. Technol.* **2008**, *68*, 3087.
- (7) Wang, Y.; Iqbal, Z.; Mitra, S. *Carbon* **2006**, *44*, 2804.
- (8) Gannon, C. J.; Cherukuri, P.; Yakobson, B. I.; Cognet, L.; Kanzius, J. S.; Kittrell, C.; Weisman, R. B.; Pasquali, M.; Schmidt, H. K.; Smalley, R. E.; Curley, S. A. *Cancer* **2007**, *110*, 2654.
- (9) Roberts, J. A.; Imholt, T.; Ye, Z.; Dyke, C. A.; Price, D. W.; Tour, J. M. *J. Appl. Phys.* **2004**, *95*, 4352.
- (10) Walton, D.; Boehnel, H.; Dunlop, D. J. *J. Appl. Phys. Lett.* **2004**, *85*, 5367.
- (11) Guo, W. L.; Guo, Y. F. *Phys. Rev. Lett.* **2003**, *91*, 115501.
- (12) Wu, J. H.; Kong, L. B. *J. Appl. Phys. Lett.* **2004**, *84*, 4956.
- (13) Shi, S.; Liang, J. *Nanotechnology* **2008**, *19*, 255707.
- (14) Song, W. L.; Cao, M. S.; Hou, Z. L.; Yuan, J.; Fang, X. Y. *Scr. Mater.* **2009**, *61*, 201.
- (15) Benitez, R.; Fuentes, A.; Lozano, K. J. *Mater. Process. Technol.* **2007**, *190*, 324.
- (16) Li, N.; Huang, Y.; Du, F.; He, X. B.; Lin, X.; Gao, H. J.; Ma, Y. F.; Li, F. F.; Chen, Y. S.; Eklund, P. C. *Nano Lett.* **2006**, *6*, 1141.
- (17) Greil, P. *Adv. Eng. Mater.* **2000**, *2*, 339.
- (18) An, L. A.; Riedel, R.; Konetschny, C.; Kleebe, H. J.; Raj, R. J. *Am. Ceram. Soc.* **1998**, *81*, 1349.
- (19) Riedel, R.; Passing, G.; Schonfelder, H.; Brook, R. J. *Nature* **1992**, *355*, 714.
- (20) Hermann, A. M.; Wang, Y. T.; Ramakrishnan, P. A.; Balzar, D.; An, L. N.; Haluschka, C.; Riedel, R. J. *Am. Ceram. Soc.* **2001**, *84*, 2260.
- (21) Shah, S. R.; Raj, R. J. *Eur. Ceram. Soc.* **2005**, *25*, 243.
- (22) Lehman, J. H.; Hurst, K. E.; Singh, G.; Mansfield, E.; Perkins, J. D.; Cromer, C. L. *J. Mater. Sci.* **2010**, *45*, 4251.
- (23) An, L. N.; Xu, W. X.; Rajagopalan, S.; Wang, C. M.; Wang, H.; Fan, Y.; Zhang, L. G.; Jiang, D. P.; Kapat, J.; Chow, L.; Guo, B. H.; Liang, J.; Vaidyanathan, R. *Adv. Mater.* **2004**, *16*, 2036.
- (24) Francis, A.; Riedel, R. J. *J. Appl. Phys.* **2009**, *105*, 07A318.
- (25) Bhandavat, R.; Singh, G.; *J. Am. Ceram. Soc.*, submitted.
- (26) Hirsch, A. *Angew. Chem., Int. Ed.* **2002**, *41*, 1853.
- (27) Shah, S. R.; Raj, R. *Acta Mater.* **2002**, *50*, 4093.
- (28) Riedel, R.; Gabriel, A. O. *Adv. Mater.* **1999**, *11*, 207.
- (29) Kremer, F.; Schönhal, A. *Broadband Dielectric Spectroscopy*; Springer: Heidelberg, Germany, 2002.
- (30) Correia, N. T.; Ramos, J. J. M. *Phys. Chem. Chem. Phys.* **2000**, *2*, 5712.
- (31) Metaxas, A.; Meredith, R. *Industrial Microwave Heating*; IEEE Power Engineering Series 4; Peter Peregrinus: London, 1983.
- (32) Benedict, L. X.; Louie, S. G.; Cohen, M. L. *Phys. Rev. B* **1995**, *52*, 8541.